Loss rates of Europa's exosphere

Alice Lucchetti[a,b], Christina Plainaki[c], Gabriele Cremonese[b], Anna Milillo[c], Timothy Cassidy[d], Xianzhe Jia[e], Valery Shematovich[f]

[a] *CISAS, University of Padova, Via Venezia 15, 35131 Padova*
[b] *INAF-Astronomical Observatory of Padova, Vicolo dellOsservatorio 5, 35131 Padova, Italy*
[c] *INAF-IAPS Roma, Istituto di Astrofisica e Planetologia Spaziali di Roma, Via del Fosso del Cavaliere, 00133 Roma, Italy*
[d] *University of Colorado, Laboratory for Atmospheric and Space Physics, 1234 Innovation Dr., Boulder, CO, USA.*
[e] *Department of Atmospheric, Oceanic, and Space Sciences, University of Michigan, Ann Arbor, MI, USA*
[f] *Institute of Astronomy RAS, Moscow, Russia*

Abstract

The reactions in the exosphere of Jupiter's moon Europa are dominated by plasma-neutral interactions leading to the effective loss of the moon's neutral population. We estimate the exosphere loss rates using the updated plasma conditions at the moon's vicinity, calculated recently by Bagenal et al. (2015) on the basis previously not analyzed Galileo data. Whereas all previous studies including loss rates estimates were based on Voyager data, in the present paper, for the first time, the state to the art results by Bagenal et al. (2015) are used in order to predict the variability of the exosphere loss due to the flapping of the Jupiter's plasma sheet over the moon. We perform our investigation for three sample plasma environment cases (hot, low density; medium; cold, high density) and we also investigate the role of charge-exchange interactions between ionosphere/pickup ions and exospheric neutrals, for all of the three dominant exosphere species, namely water, oxygen and hydrogen. We find that the O_2 - O_2^+ charge-exchange process has a dominant role in the exosphere loss, contrary to what it had been previously thought. Using both the revised O_2 column density obtained from the EGEON model (Plainaki et al., 2013) and the current loss rates estimations, we find that the volume integrated loss rate due to O_2 - O_2^+ charge exchange is in the range $(13 - 51) \times 10^{26} s^{-1}$, depending on the moon's orbital phase and illumination conditions. This result is relevant to studies related to the interactions between Europa's neutral population and space environment and can be of use during the observations planning preparation for future missions to Europa.

Keywords:

1. Introduction

The exosphere of Jupiter's moon Europa includes mainly the following populations: H_2O, released mainly through ion sputtering caused by the energetic ions of Jupiter's magnetosphere that impact the moon's surface (Brown et al., 1982; Plainaki et al., 2010, 2012; Cassidy et al., 2013)

*Corresponding author
Email address: alice.lucchetti@oapd.inaf.it (Alice Lucchetti)

and secondarily through sublimation (Shematovich et al., 2005); O_2 and H_2, both species produced through chemical reactions among different products of H_2O radiolytic decomposition (Johnson, 1990; Shematovich et al., 2005; Cassidy et al., 2010; Plainaki et al., 2010, 2012, 2013); and some minor species like Na and K (Brown & Hill, 1996; Brown, 2001; Leblanc et al., 2002, 2005) and H, O, HO_2, and H_2O_2 (Baragiola, 2003). The discovery of an O_2 atmosphere was made by Hall et al. (1995, 1998) using the Hubble Space Telescope (HST) observations of ultraviolet line emission of atomic oxygen. The observed 1304/1356 emission line intensities ratio was attributed to electron impact dissociative excitation of O_2. Later, the observations of the Ultraviolet Imaging Spectrograph (UVIS) onboard Cassini confirmed the existence of a tenuous O_2 atmosphere during Cassini's flyby of Jupiter (Hansen et al., 2005). Recent observations with HST have revealed surpluses of hydrogen Lyman alpha and atomic oxygen emissions above the moon's southern hemisphere, that have been interpreted as evidence of transient vapor water plumes (Roth et al., 2014).

The understanding of the evolution of Europa's exosphere and the estimation of its total mass loss has as a mandatory prerequisite the understanding of the interactions between Jupiter's magnetospheric plasma and the satellite's neutral environment. The source processes responsible for the generation of the exosphere of Europa as well as the chemistry between exospheric neutrals and Jupiter's magnetospheric plasma have been discussed many times in the past (see in Plainaki et al. (2012, 2013); Cassidy et al. (2010, 2013); Krupp et al. (2010); Dalton et al. (2010); Coustenis et al. (2010); Bagenal et al. (2004); Pappalardo et al. (2009)). In particular, the plasma-neutrals interactions have been mainly studied either on the basis of Voyager and Galileo flyby data (Kabin et al., 1999; Bagenal et al., 2004; Schilling et al., 2008; Lipatov et al., 2010) or through analytical (Saur et al., 1998) and Monte Carlo models (Shematovich et al., 2005; Smyth & Marconi, 2006; Plainaki et al., 2012). However, the lack of a sufficient series of in situ measurements able to: a) further constrain the estimations obtained through the above mentioned studies and b) determine the variability of the magnetospheric plasma properties around Europa, has significantly limited our knowledge on the plasma-neutrals interactions and the temporal and spatial variability of the exosphere loss rates. On the other hand, our understanding of the exosphere sources has been significantly expanded by the results of a series of related laboratory ice experiments (Brown et al., 1978; Baragiola, 2003; Teolis et al., 2015; Galli et al., 2015). Nevertheless, a thorough and detailed determination of the balance between exosphere sources and losses is expected to come once new in situ data will be obtained (i.e. during the ESA/JUICE and NASA/Europa missions).

In view of preparation for future missions to Europa, an accurate estimation of the loss rates for the main constituents of the exosphere of Europa, based on state to the art models providing the plasma-properties nearby the satellite as well as on laboratory derived cross sections for different plasma-neutral interactions, is of significant help. The scope of this paper is to provide detailed estimations of the loss rates of Europa's exosphere, based on the updated plasma conditions at the moon's vicinity, calculated recently by Bagenal et al. (2015) on the basis of previously not analyzed Galileo data. In particular, in the current paper we provide a broad and long list of reactions, not discussed thoroughly in previous Monte Carlo modeling papers, and we estimate for the first time their impact to the Europa's neutral environment for three sample plasma environment cases (hot, low density; medium; cold, high density). All previous studies including estimations of the loss rates of Europa's exosphere were based: a) on Voyager-1 data (e.g. Sittler & Strobel, 1987) or b) Cassini data (Delamere et al., 2005) or c) on plasma properties information provided by the earlier Bagenal (1994) model (e.g. Saur et al., 1998; Smyth & Marconi, 2006; Shematovich et al., 2005; Plainaki et al., 2012, 2013). Contrary to these studies, in the present paper, for the first time, the state to the art results by Bagenal et al. (2015) are used in order to predict the variability of the exosphere

loss, due to the flapping of the Jupiter's plasma sheet (JPS) over the moon. The motivation for this work, therefore, is to provide an add-on to current knowledge, which can be further used as a resource for the improvement of future plasma and exosphere models. Additionally, we investigate the role of different charge-exchange interactions between ionosphere/pickup ions and exospheric neutrals, for all three dominant exosphere species, namely water, oxygen and hydrogen, an issue that had been studied only marginally in the past (see works by Shematovich et al. (2005); Smyth & Marconi (2006)). For completeness, we provide information also on photoreactions for both cases of quiet and active Sun. The paper is organized as follows: in Section 2, the estimations of the loss rates of Europa's exosphere, based on recent literature values of the efficiency of the actual processes and plasma properties around the moon, are provided. In Section 3, we compare our results with those of previous calculations and we discuss them in the context of future in situ measurements during the ESA's JUICE mission. Finally, in Section 4, the conclusions of the current study are given. At the current moment, an accurate estimation of the loss rates for the main constituents of the exosphere of Europa, based on the existent literature on the plasma-properties nearby the satellite as well as on interactions cross sections, may be help for the modeling of the moon's neutral providing necessary quantitative inputs.

2. Loss processes: rates and variability

The interactions between Jupiter's magnetospheric plasma and the solar UV radiation with Europa's neutral environment lead in general to ionization and/or dissociation of the exosphere constituents. As a result, a population of fresh ions can be produced and supply the plasma, contributing, in this way, to the further ionization of the neutral environment; moreover, the freshly dissociated molecules modify the composition of the exosphere creating inhomogeneities in the nominal neutral distribution around the moon. Interactions in the near-Europa space environment, therefore, result in both dynamical changes of the plasma composition and temperature and effective exosphere loss.

2.1. Plasma-neutral interactions

The cross sections relative to plasma-neutral interactions are energy dependent hence the respective loss rates depend on the speed distribution of the plasma, as well as the densities of each reactant (Burger et al., 2010). Therefore, in order to address the role of the different loss mechanisms, the external plasma environment has to be considered first.

The plasma properties in the space environment in which Europa is embedded have been identified in detail in the past through the plasma model by Bagenal (1994), which was based on Voyager-1 Ultraviolet Spectrometer (UVS) data (Shemansky, 1987; Bagenal et al., 1992) and plasma instrument (PLS) measurements at the orbit of Io. According to this model, the plasma electron population at Europa's orbit includes a core cold and a hot component that can be approximated by two Maxwellian distributions (at 20 and 250 eV, respectively). Moreover, the plasma properties were shown to have a variability depending on the location of Europa with respect to the JPS. In particular, due to the tilted (with respect to JPS) orbit of Europa, the plasma density falls off north/south of above/below the centrifugal equator with a scale height of $\sim 1R_J$ for 50-100 eV plasma (Kivelson et al., 2004). As Europa moves in its orbit, it effectively moves up and down the JPS and the density and temperature of the local plasma change remarkably. The Bagenal (1994) model predicted for the electron density at the orbit of Europa values of $\sim 35 - 40\ cm^{-3}$ off the equator and values of $80 - 100\ cm^{-3}$ near it, depending on the strength of the equatorial current.

Observed electron densities over Galileo flybys of Europa ranged from 18 cm^{-3} to 250 cm^{-3} (Gurnett et al., 1998; Kurth et al., 2001). Ion-mixing ratios in the vicinity of Europa were estimated by Delamere et al. (2005) on the basis of the Cassini Ultraviolet Imaging Spectrograph (UVIS) data (Steffl et al., 2004). We note that the earlier models based on analyses of Voyager UVS data had lower abundances of S_2^+ and higher abundances of O^+ than the ones estimated by (Steffl et al., 2004). Recently, Bagenal et al. (2015) analyzed the available Galileo PLS and Plasma Wave Instrument (PWS) data to derive electron density, azimuthal speed and ion temperature of the plasma in the space environment near Europa. They found that the flow speed has a narrow distribution around a median value that is equal to 83% of the corotation speed. Moreover, Bagenal et al. (2015), based on the composition derived by Delamere et al. (2005), provided three cases of plasma conditions in the near-Europa space: (a) Low density, high temperature; (b) Medium conditions of density and temperature; and (c) high density, low temperature. A dipole field geometry and a longitude (112° or 292° System III longitude) where magnetic, centrifugal and rotational equators are aligned, were assumed (Bagenal et al., 2015). The updated plasma electron and ion conditions in the near-Europa space environment, as given in Bagenal et al. (2015), are used in the exosphere loss estimations in the current paper and provided in Table 1.

Whereas the available in situ measurements guide the construction of plasma torus models in the near Europa space environment, the plasma properties in the near surface regions are currently known with less certainty and they are mainly provided by models. 3D hybrid kinetic models (Lipatov et al., 2010, 2013, e.g) or 3D MHD models (Schilling et al., 2007; Rubin et al., 2015) of plasma interaction have been developed so far in order to provide some insights of the near surface plasma environment. Although a) strong evidence for the existence of an ionosphere has been provided through the Galileo Radio Science observations (Kliore et al., 1997) and b) so far substantial progress in modeling has been made, there are still substantial uncertainties considering the specific characteristics (e.g. height and thickness) of an ionosphere layer between the impinging magnetospheric ions and the moon's surface. Indeed, Sittler et al. (2013) discussed the complexity of inferring Europa's ionospheric scale height from Galileo Radio Science observations and concluded that the inferred electron density should be interpreted combining also the knowledge obtained through a global interaction model (e.g. Lipatov et al., 2010). Moreover, these authors noted that several plasma modeling efforts of the past could not resolve the problem of determining the characteristics of the ionopause due to either the modeling technique itself (for example the MHD models by Schilling et al. (2007, 2008) assumed intrinsically zero gyroradius for the ions) or due to low model-resolution (for example, equal to $\sim$ 150 km in the model by Lipatov et al. (2010)).

Understanding the characteristics of Europa's ionosphere is of significant importance in order to determine the exosphere loss rates. In general, in a planetary (or lunar) atmosphere, below the ionopause, i.e. the transitional region between ions of magnetospheric origin and ionospheric ions, the external plasma does not penetrate, the convective electric field of the external flow is near zero and the gyroradius of the local ions is essentially zero. At altitudes above the ionopause the pick-up ions dominate, the plasma flow is non-zero and the convective electric field will be relatively large. If the thickness of the ionopause is large with respect to its height then the ionopause does not occur and the external plasma flow can penetrate down to the moon's surface. Recent simulations by Sittler et al. (2013) showed that at Europa the plasma flow can extend down near the surface when the O_2 column density is low enough. In particular, they showed that for a column density equal to $\sim 5 \times 10^{14} cm^{-2}$ the plasma flow stopped essentially at the altitude of 40 km defined as the height of the occurrence of the ionopause. Moreover, the model by Sittler et al. (2013) provides the density profile of pick up ions of different species for altitudes up to 200 km from the surface

(see in Sittler et al. (2013), Fig.9). The ionosphere and pick up ion properties provided by Sittler et al. (2013) are used in the current paper in order to estimate the exosphere loss rates.

Based on the above description, the interactions, between the plasma and Europa's exosphere leading to the actual loss of the neutral population, refer either to electron-neutral or to ion-neutral collisions. In the latter case, the interactions refer (potentially) to three ion populations, namely the ions in the plasma torus (with origin from Io), dominating at altitudes $\geq$ 200 km; the ionosphere ions, originating from the ionization of the sputtered neutral exosphere, dominating at altitudes $\leq$ 40 km; the pick-up ions, being the ionized neutrals that once generated they are immediately accelerated and picked-up by the corotating magnetic field. The term potential refers to the uncertainty for the existence of an ionosphere layer at Europa. In the current paper, we estimate the loss rates corresponding to electron and ion interactions with the neutral exosphere for the three plasma torus conditions given in Table 1 and the main ionosphere and pick up ion populations provided in Sittler et al. (2013). In the current paper we consider only the main constituents of Europa's exosphere, namely H_2O, O_2 and H_2. Although the expected ice irradiation processes at Europa do not exclude the existence of some other less abundant exosphere species, such as OH and H (Watanabe et al., 2000) or H_2O_2 and HO_2 (Kimmel et al., 1994; Orlando & Kimmel, 1997), laboratory measurements of ice irradiation experiments have shown that water molecules dominate the total release yield at lower temperatures ($<$ 120 K) and molecular oxygen and hydrogen at higher ($>$ 120 K) temperatures (Johnson & Kanik, 2001).

Table 1: Plasma properties in the near-Europa space environment as estimated by Bagenal et al. (2015) on the basis of previously unprocessed data. The ion composition is based on the physical chemistry model by Delamere et al. (2005)

.

	PLASMA CONDITION:	**(1) Low/Hot**	**(1) Medium**	**(1) High/Cold**	**Note**
$\boldsymbol{T(S^+)(eV)}$	S^+ temperature	500	130	70	
$\boldsymbol{T(S^{2+})(eV)}$	S^{2+} temperature	250	65	40	
$\boldsymbol{T(S^{3+})(eV)}$	S^{3+} temperature	170	45	25	
$\boldsymbol{T(O^+)(eV)}$	O^+ temperature	500	130	70	
$\boldsymbol{T(O^{2+})(eV)}$	O^{2+} temperature	340	90	50	
$\boldsymbol{T(H^+)(eV)}$	H^+ temperature	70	17	10	
$\boldsymbol{T_i}$ **(eV)**	ion temperature	340	88	48	from the Galileo/PLS instrument
$\boldsymbol{V(km/s)}$	flow speed	123	98	76	from the Galileo/PLS instrument
$\boldsymbol{T_e}$ **cold (eV)**	electron temperature (cold component)	30	20	10	
$\boldsymbol{T_e}$ **hot (eV)**	electron temperature (hot component)	1200	300	200	
$\boldsymbol{N_e cm^{-3}}$	(cold) electron density	63	158	290	from the Galileo/PLS instrument
$\boldsymbol{N_e(hot)/N_e}$	hot to cold electron density ratio	0.1	0.05	0.02	
$\boldsymbol{N(S^+)/N_e}$	S^+ composition	0.02	0.02	0.02	Delamere et al. (2005)
$\boldsymbol{N(S^{2+})/N_e}$	S^{2+} composition	0.14	0.14	0.14	Delamere et al. (2005)
$\boldsymbol{N(S^{3+})/N_e}$	S^{3+} composition	0.04	0.04	0.04	Delamere et al. (2005)
$\boldsymbol{N(O^+)/N_e}$	O^+ composition	0.3	0.3	0.3	Delamere et al. (2005)
$\boldsymbol{N(O^{2+})/N_e}$	O^{2+} composition	0.08	0.08	0.08	Delamere et al. (2005)
$\boldsymbol{N(H^+)/N_e}$	H^+ composition	0.12	0.12	0.12	Delamere et al. (2005)
$\boldsymbol{< A_i >}$	assumed mass of the dominant heavy ion species (amu)	18	18	18	Delamere et al. (2005); Bagenal et al. (2015)
$\boldsymbol{< Z_i >}$	assumed charge of the dominant heavy ion species (amu)	1.5	1.5	1.5	Delamere et al. (2005); Bagenal et al. (2015)
$\boldsymbol{B(nT)}$	background magnetic field	480	450	423	Delamere et al. (2005); Bagenal et al. (2015)

2.1.1. Electron-neutral interactions

Plasma electrons impacting the exosphere of Europa can dissociate and/or ionize its various constituents. The dissociation (or ionization) rate due to electron impact processes is computed by

$$\nu_e = \kappa(V_e) N_e \tag{1}$$

where N_e is the electron density and κ is the rate coefficient of the reaction (in $cm^3 s^{-1}$), determined from the cross section of the reaction and the velocity distribution function $f(V_e)$, where (V_e) is the velocity of the electrons measured relative to the neutrals. For electron impact processes, the plasma flow speeds (also called bulk velocities) can be ignored since the electron thermal speeds are much larger. For example, cold 20 eV electrons (Medium case in Table 1) have velocities of $\sim 2.7 \times 10^3$ km/s which are much larger than the measured flow speed in the near-Europa space, equal to 98 km/s (Bagenal et al., 2015). Therefore, for a thermalized (Maxwellian) electron population, the rate coefficient is a function of the electron temperature:

$$\kappa(T_e) = \int f(V_e)\sigma(V_e) dV_e \tag{2}$$

where $f(V_e)$ is the velocity distribution function of the electron population and σ is the experimentally determined cross section of the reaction. In order to estimate κ, we approximately consider the mean electron velocity $< V_E >= \frac{2}{\sqrt{\pi}} \sqrt{\frac{2k_b T_e}{m_e}}$ of a Maxwellian distribution function. Our results for different plasma electron populations are resented in Table 2.

2.1.2. Ion-neutral Interactions

Ion-neutral reactions refer to collisions between plasma ions and neutral species. The charge-exchange (also called "charge transfer") is a collisional process that takes place during the interaction between a relatively fast (energetic) ion and a cold neutral. During this process the fast ion and the cold neutral exchange their charge hence an energetic neutral atom (ENA) and a cold ion are being formed. In case the projectile and the target particles are of the same species, charge exchange is a symmetrical resonance process (Hasted & Hussain, 1964); in case of different species, it could be an accidental resonance process (for example, H^+ projectile and O (Stebbings et al., 1964) or H_2 (Hasted & Hussain, 1964) targets). In these cases, only a few eV are lost during the interaction, and the newly created ENA retains approximately both the energy of the colliding energetic ion and its direction (Milillo et al., 2005). If the mean free path of the newly created ENAs is long enough, such an ENA can transport information out of the generation region, thus allowing remote sensing of the interaction process (e.g. Roelof et al., 1985; Roelof, 1987; Daglis & Livi, 1995; Orsini & Milillo, 1999; Barabash et al., 2001; Milillo et al., 2001; Orsini et al., 2001).

Charge-exchange rates are also determined by Equation 1 and 2 substituting the electron density and velocity, with the ion density N_i and velocity relative to the neutrals (V_i), respectively. Contrary to the electron-neutral interaction case, the relative bulk motion between the ions and neutrals is significant hence it needs to be taken into account when calculating the respective reaction cross section. The charge-exchange rate coefficient is given by:

$$\kappa(V_i) = \int f(V_i)\sigma(V_i) dV_i \tag{3}$$

where $V_i = V - V_{orb}$, with V_{orb} being the orbital velocity of Europa, equal to 14 km/s, and V being the flow velocity of the plasma as derived from the Galileo PLS measurements (Bagenal et al.,

2015). We note that if the thermal temperature is large then both the thermal (random) motions of the ions and the bulk motion of the plasma relative to the neutral gas must be considered. This is the case of plasma being slowed as flowing through satellite exospheres or the Enceladus plume (Burger et al., 2010). Johnson et al. (2006) showed that the presence of H_3O^+ in the Saturnian plasma implied reactions between neutral and ionized water molecules at low relative velocities because the cross section for H_3O^+ production is large for speeds below ~ 10 km/s (Lishawa et al., 1990). For the Europa case, the random thermal ion velocities estimated by Bagenal et al. (2015) are in general lower than the flow velocity hence in the current study we do not take their effect to the relative velocity into account. Future in situ measurements of course will provide more detailed information on the plasma properties in the near-surface environment of Europa allowing hence a more accurate evaluation of the rates of the plasma-neutral interactions.

In our loss rate estimates corresponding to the interactions between the plasma torus ions and the neutrals (see Table 3), we take into account only the S^{++} and O^+ ions, since they are the dominant species of the sub-corotating plasma, with densities equal to 15% and 20% of the electron density, as inferred from UV observation in Steffl et al. (2004), in consistency also with the model by Delamere et al. (2005). We underline that the low energy plasma composition was not measured directly by Galileo but it was inferred through the spectra and Mach numbers of the measured flows (Sittler et al., 2013). Indeed these measurements could not distinguish O^+ from S^{++} hence the relative abundances for these species are currently known only on the basis of models. The complete composition of the plasma in the near-Europa space environment is presented in Table 1. We note that in the model of Delamere et al. (2005) the proton density ($\sim 12\%$ of the electron density) is derived as additional ion charge to match electron density and to satisfy charge neutrality. Since the H^+ composition is not a direct measurement, in the current study we do not estimate rates corresponding to plasma neutral reactions involving H^+. Our results are presented in Table 3.

Regarding the loss rate estimates corresponding to the interactions between the ionosphere ions and the neutrals, we attempt to provide an upper limit of the respective charge-exchange reactions considering the O_2^+, H_2O^+, and H_2^+ ionosphere densities at the height of the ionopause (where they become maximum). Considering the interactions between pick-up ions and exosphere, in the current paper we provide estimations for altitudes > 200 km, since the region between the height of 200 km and the ionopause is a transition region where the density of the pick-up ions is highly variable (see Sittler et al. (2013), Fig. 9). For the pick-up ions at the altitude of 200 km we assume a relative speed equal to the one of the plasma torus (see Table 1). We underline that our estimated loss rates due to pick-up ion interactions are in consistency with the overall plasma neutrality. Note that Delamere et al. (2005) estimated that whereas the addition of pickup O^+ ions and O_2^+ ions to the torus increases the net temperature from 130 eV and 100 eV to 300 eV and 200 eV respectively, the modification they bring to the plasma torus composition is minor. For the ionospheric ions, originating from the ionization of the sputtered neutral exosphere and dominating at altitudes $<$ 40 km, we assume a velocity equal to ~ 10 km/s as given by Sittler et al. (2013). Our results are presented in Table 4. Although we did not perform any detailed calculations corresponding to the transition region between the ionopause and the altitude at which the plasma torus becomes dominating (assumed to be equal to ~ 200 km, as in Sittler et al. (2013)), we expect that the respective loss rates will vary between the values provided in Table 3 and Table 4.

.

Table 2: Electron impact reactions rates for different plasma conditions

Reaction	**(1) Low/Hot**		**(2) Medium**		**High/Cold**		**Note**
			$\boldsymbol{\nu(10^{-6}s^{-1})}$				
	cold	**Hot**[a]	**Cold**	**Hot**	**Cold**	**Hot**	
$H_2O + e \rightarrow OH + H + e$	3.0		3.31	1.28	0.92	0.96	[1,2]
$H_2O + e \rightarrow H_2O^+ + 2e$	1.88	0.58			0.18[b]	0.61	[2]
$H_2O + e \rightarrow OH^+ + H + 2e$	0.37	0.19	1.94	0.84		0.2	[2]
$H_2O + e \rightarrow OH + H^+ + 2e$	0.99	0.15	0.069	0.28		0.19	[2]
$H_2O + e \rightarrow H_2 + O^+ + 2e$	0.0085	0.026	0.013	0.26		0.039	[2,3]
$O_2 + e \rightarrow O + O + e$	1.43		0.0014	0.05	1.57[b]	0.16[c]	[4]
$O_2 + e \rightarrow O_2^+ + 2e$	1.5	0.79	2.58		0.082[b]	0.76[c]	[4]
$O_2 + e \rightarrow O^+ + O + 2e$	0.28	0.42	1.18	1.1		0.47[c]	[5]
$H_2 + e \rightarrow H + H + e$	1.24		0.091	1.66	3.55		[6]
$H_2 + e \rightarrow H_2^+ + e$	1.48	0.27	3.55		1.32	0.45	[7]
$H_2 + e \rightarrow H^+ + H + 2e$	0.019	0.016	1.32	0.45	0.024	0.036	[7]

[a] The cross section for the hot electron population are reported for an energy equal to 1000 eV (instead of 1200 eV) because cross sections for higher electron temperature are not reported in [2,3].

[b] The cross section are reported for an energy equal to 13.5 eV.

[c] The cross section are reported for an energy equal to 198 eV.

Reaction 1 Cross sections measured over an energy range from threshold to 300 eV [1].

Reaction 2,3,4,5 Reaction cross section measured from threshold to 1000 eV [2, 3].

Reaction 6 Cross sections measured over an energy range from 13.5 eV to 198.5 eV [4].

Reaction 8 Cross section corresponding to an electron temperature of 10 eV is below the threshold [5].

Reaction 9 Cross sections measured over an energy range from 9 eV to 80 eV [6].

Reaction 10,11 Cross sections measured over an energy range from threshold to 1000 eV [7].

Table References: [1] Harb et al. (2001a); [2] Itikawa & Mason (2005); [3] Shirai et al. (2001); [4] Cosby (1993); [5]Itikawa (2009); [6] Yoon et al. (2008); [7] Straub et al. (1996).

Table 3: Plasma flow charge exchange reactions rates given for reactions between S^{++} and O^{+} ions and O_2, H_2 and H_2O neutrals. The ion velocity is equal to $V - V_{orb}$, where V_{orb} is the orbital velocity of Europa (equal to 14 km/s) and V is the flow velocity of the plasma as derived from the Galileo PLS measurements (Bagenal et al., 2015). The S^{++} and O^{+} ion densities used to calculate the reaction rates are based on the physical chemistry model by Delamere et al. (2005), see Table 1.

	(1) Low/Hot	**(2) Medium**	**High/Cold**	**Note**
V_{ions} (km/s)	109	84	62	[1]
$N(S^{++})$ cm^{-3}	9	22	41	[2]
$N(O^{+})$ cm^{-3}	19	47	87	[2]
Reaction	$\boldsymbol{\nu(10^{-6}s^{-1})}$	$\boldsymbol{\nu(10^{-6}s^{-1})}$	$\boldsymbol{\nu(10^{-6}s^{-1})}$	
$S^{++} + O_2 \rightarrow S^{+} + O_2^{+}$	0.15	0.28	0.38	[3]
$O^{+} + O_2 \rightarrow O + O_2^{+}$	0.27	0.51	0.7	[3]
$S^{++} + H_2 \rightarrow S^{+} + H_2^{+}$	0.09	0.32	0.42	Copy of the below
$O^{+} + H_2 \rightarrow O + H_2^{+}$	0.09	0.32	0.42	[4]
$S^{+} + +H_2O \rightarrow S^{+} + H_2O^{+}$				
$O^{+} + H_2O \rightarrow O + H_2O^{+}$		0.7	0.11	[5]

Reaction 3 The cross section is not available and we used the value of the cross section of the reaction below (as Dols et al. submitted).
Reaction 5 Cross section value not found in literature.
Reaction 6 Cross section studied in the energy range 1 to 400 eV.
Table References: [1] Bagenal et al. (2015); [2] Delamere et al. (2005); [3] McGrath & Johnson (1989); [4] Tawara et al. (1985); [5]Turner & Rutherford (1968).

Table 4: Pick up and ionosphere charge exchange reactions rates given for reactions between O_2^+, H_2^+ and H_2O^+ ions and O_2, H_2 and H_2O neutrals. We assume for pick up ions a relative speed equal to the one of the plasma torus. The pick up ion density is provided by Sittler et al. (2013) (Figure 9) and it is equal to 10 cm^{-3} for the three ions species (O_2^+, H_2^+, H_2O^+), which is valid for the different plasma condition cases. The ionosphere ion velocity (10 km/s) and the ionosphere ion density are provided by Sittler et al. (2013). We assume an ion density equal to 10000, 50 and 25 cm^{-3} for O_2^+, H_2^+, H_2O^+ ions respectively.

	PICK UP IONS			**IONOSPHERE**	**Note**
	(1) Low/Hot	**(2) Medium**	**High/Cold**		
V_{ions} (km/s)	109	84	62	10	[1] pick up ions, [2] ionosphere ions
$N(O_2^+)cm^{-3}$	10	10	10	1000	[2]
$N(H_2^+)cm^{-3}$	10	10	10	50	[2]
$N(H_2O^+)cm^{-3}$	10	10	10	25	[2]
Reaction	$\boldsymbol{\nu(10^{-6}s^{-1})}$	$\boldsymbol{\nu(10^{-6}s^{-1})}$	$\boldsymbol{\nu(10^{-6}s^{-1})}$	$\boldsymbol{\nu(10^{-6}s^{-1})}$	
$O_2^+ + O_2 \rightarrow O_2 + O_2^+$		0.05	0.04	15	[3]
$H_2^+ + O_2 \rightarrow H_2 + O_2^+$	0.027	0.027	0.027	1.35	[4]
$H_2O^+ + O_2 \rightarrow H_2O + O_2^+$	0.002	0.002	0.002	0.005	[5]
$O_2^+ + H_2 \rightarrow O_2 + H_2^+$	0.066	0.034	0.019	0.005	[6,7]
$H_2^+ + H_2 \rightarrow H_2 + H_2^+$	0.082	0.067	0.054	0.12	[8]
$H_2O^+ + H_2 \rightarrow H_2O + H_2^+$					
$O_2^+ + H_2O \rightarrow O_2 + H_2O^+$					
$H_2^+ + H_2O \rightarrow H_2 + H_2O^+$	0.44	0.42	0.36		[9]
$H_2O^+ + H_2O \rightarrow H_2O + H_2O^+$				0.025	[10]

Reaction 1 Cross section measured for energy up to 1000 eV [3].
Reaction 2,3 The reaction rate coefficients for references [4,5] are published for a fixed gas temperature or a limited range of temperatures. These values are equal to 2.7×10^{-9} and 0.2×10^{-9}, which are reported from [4] and [5] respectively.
Reaction 4 Cross section measured from 100 eV [6,7].
Reaction 6,7 Values not found in literature.
Reaction 8 Cross section measured for incident ion energy range 30 - 500 eV.
Reaction 9 Cross section measured for energy up to 60 eV.
Table References: [1] Bagenal et al. (2015); [2] Sittler et al. (2013); [3] Benyoucef & Yousfi (2014); [4] Kim & Huntress (1975); [5]Fehsenfeld et al. (1967); [6]Irvine & Latimer (1997); [7]Hasan & Gray (2007); [8]Vance & Bailey (1966); [9]Coplan & Ogilvie (1970); [10]Lishawa et al. (1990).

2.2. Photoreactions

Photoreaction rates are given at 1 UA by Huebner et al. (1992). These rates are inversely proportional to the distance of Europa from the Sun squared. The values listed in Table 5 are for quiet and active Sun at Europa's orbit (5.2 UA) for H_2O, O_2 and H_2 Photo-Reactions.

For completeness, we mention the contribution coming from fresh photoelectrons that have enough energy to dissociate and ionize the neutrals. We estimate that the rate resulting from this secondary process is about 10% - 30% of the photoreaction rate. This is a standard approximation used in the aeronomic studies, that was checked and validated in the accurate calculations of the photo and photoelectron rates for different planetary atmospheres (see, for example, Hubert et al. (2012) and Ionov et al. (2014)).

Table 5: Photoreaction rates for H_2O, O_2 and H_2 from Huebner et al. (1992).

Photo-Reaction	$\nu(10^{-6}s^{-1})$
$H_2O + h\nu \rightarrow H + OH$	$0.38 - 0.65$
$H_2O + h\nu \rightarrow H_2 + O(^1D)$	$0.022 - 0.055$
$H_2O + h\nu \rightarrow H + H + O$	$0.028 - 0.71$
$H_2O + h\nu \rightarrow H_2O^+ + e$	$0.012 - 0.031$
$H_2O + h\nu \rightarrow OH^+ + H + e$	$0.0021 - 0.0056$
$H_2O + h\nu \rightarrow OH + H^+ + e$	$0.00048 - 0.0015$
$H_2O + h\nu \rightarrow H_2 + O^+ + e$	$0.00022 - 0.00082$
$O_2 + h\nu \rightarrow O(^3P) + O(^3P)$	$0.0052 - 0.0082$
$O_2 + h\nu \rightarrow O(^3P) + O(^1D)$	$0.15 - 0.24$
$O_2 + h\nu \rightarrow O(^1S) + O(^1S)$	$0.0015 - 0.0035$
$O_2 + h\nu \rightarrow O_2^+ + e$	$0.017 - 0.044$
$O_2 + h\nu \rightarrow O + O^+ + e$	$0.004 - 0.013$
$H_2 + h\nu \rightarrow H(^1S) + H(^1S)$	$0.0018 - 0.004$
$H_2 + h\nu \rightarrow H(^1S) + H(2s, 2p)$	$0.0013 - 0.003$
$H_2 + h\nu \rightarrow H_2^+ + e$	$0.002 - 0.004$
$H_2 + h\nu \rightarrow H + H^+ + e$	$0.00035 - 0.0011$

3. Discussion

For the H_2O exosphere we find that the dominant loss is due to electron impact dissociation. As shown in Table 2, such process is expected to have an efficiency that varies with the assumed plasma conditions (i.e. density and temperature). We note that such plasma conditions (taken from the Bagenal et al. (2015) model) depend on both the location of Europa with respect to the JPS and on the epoch of the Galileo observations on which the plasma model was based. Maximum loss is expected for the orbital phases of median plasma conditions (Case (2) in Table 2) and it is estimated to be equal to $3.31 \times 10^{-6} s^{-1}$. Production of minor species H and OH is favoured during these phases. We note that the cold plasma electron population is the main responsible for the H_2O exosphere loss.

For the H_2 exosphere we find that the dominant loss process is electron impact ionization (leading to the production of H_2^+) when Europa is under median plasma conditions, and electron impact dissociation when Europa is found under conditions of high plasma density and low plasma temperature (Case (3) in Table 2). Both processes have a rate equal to $3.55 \times 10^{-6} s^{-1}$. The dissociation process populates the exosphere with H atoms that, given their low mass, can easily escape the moon's gravity and make part of Europa's neutral cloud (gravitationally bounded to Jupiter).

For the O_2 exosphere, we find that charge-exchange reactions between the ionospheric O_2^+ and exospheric O_2 molecules have the highest rates with respect to all other loss process. In particular, we find that the $O_2^+ - O_2$ reaction rate, equal to $\sim 15 \times 10^{-6} s^{-1}$ is by a factor of ~ 6 and ~ 10 higher than the ones corresponding to electron impact ionization (medium case in Table 2) and electron impact dissociation (High/cold case in Table 2) processes, respectively. As in case of H_2O and H_2 exospheres, also here the efficiency of the electron impact processes depends strongly on the position of Europa with respect to the JPS determining the actual plasma conditions. In particular, the electron impact ionization loss rate varies by a factor up to ~ 3.4 and the dissociation rate by a factor up to ~ 31 among the three considered cases of plasma conditions. Although these processes are not the ones determining the actual loss of exosphere molecules, their rates can be used in order to roughly estimate the production of ionosphere O_2^+ and atomic oxygen. Information on such intermediate products of the plasma-neutral interactions, however minor, can be useful during the interpretation of remote sensing measurements of Europa's exosphere (as for example: the ultraviolet line emission of atomic oxygen).

In order to calculate the volume integrated neutral loss rates we use the exosphere described by the EGEON model (Plainaki et al., 2012, 2013), including the release yields revised described in Plainaki et al. (2015). We consider two different configurations between Jupiter, Europa and the Sun: a) subsolar point coincides with the leading hemisphere apex (corresponding to Conf.-1 in Plainaki et al. (2013)) and b) subsolar point coincides with the trailing hemisphere apex (corresponding to Conf.-3 in Plainaki et al. (2013)). For case (a) the spatially averaged O_2 column density given by the revised EGEON model is equal to $2.7 \times 10^{18} m^{-2}$ whereas for case (b) it is equal to $1.1 \times 10^{19} m^{-2}$. The O_2 volume integrated loss rates due to the dominant loss mechanisms (these are charge-exchange, electron impact ionization and electron impact dissociation, in order of efficiency) are presented in Table 6. For comparison, in Table 6, we also present the results obtained through other studies. The respective volume integrated loss rates calculated through different models are also presented. We note that in our estimations, the volume integrated loss rates are proportional to the neutral column density hence the difference in their values for different exosphere configurations will be due to linear scaling.

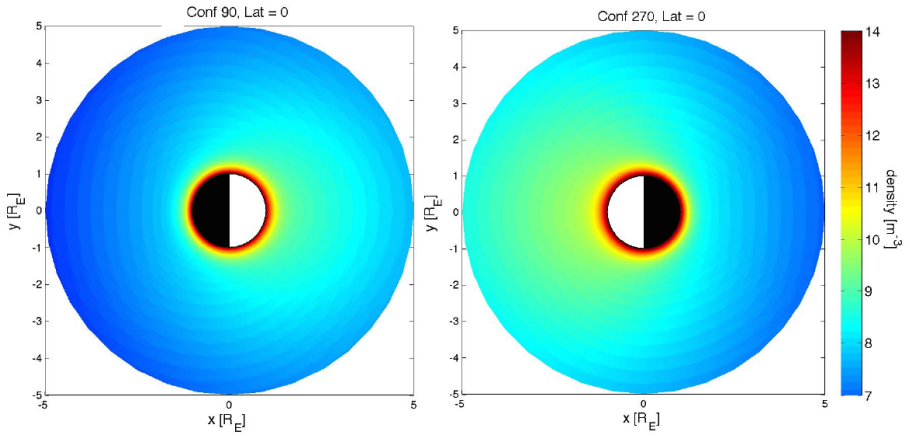

Figure 1: map of the O_2 volume density from the analytical model of Milillo et al. (submitted) derived from the EGEON model of Plainaki et al. (2013)

Table 6 shows that the ionosphere plasma-neutral interaction is the most important agent for the exospheric O_2 depletion. However, we note that the estimated rates corresponding to charge-exchange presented in Table 6 do not represent a net exosphere loss, necessarily. This is because of the following reason. A single charge-exchange reaction results in the loss of a relatively cold O_2 exospheric molecule (via charging) and to a production of an energetic O_2 molecule; the latter will leave the Europa gravity field only if its velocity is bigger than the gravitational escape velocity and if its direction is not pointing versus the surface. We can assume that the first condition is satisfied almost always since the O_2^+ velocity (in the current study assumed to be equal to $\sim$ 10 km/s, following Sittler et al. (2013) is generally larger than the gravitational escape velocity (equal to $\sim$ 2.02 km/s) and since this collisional process can be considered elastic. The second condition, however, is not necessarily satisfied during every reaction because it depends on the relative velocities directions between the initial ions and the exospheric neutrals. Therefore, the net exosphere loss rate due to charge exchange for the exosphere will result from the balance between the gain due to the freshly generated energetic O_2 molecules (i.e those that do not escape Europa's gravity field) and the loss due to the freshly ionized O_2. Recently, Dols et al. (submitted) modeled symmetrical charge-exchange cascades between ionospheric O_2^+ and exospheric O_2 and showed that the total production rate of ejected neutrals could be even an order of magnitude larger than the production of ions. In the current calculation, we make the rough assumption that at least half of the fresh energetic O_2 molecules produced through charge-exchange have velocities directions favouring escape. In this case, we deduce that the expected loss of the exospheric O_2 due to charge-exchange has values equal to 1/2 of the ones presented in Table 6 hence ranging between $6.5 \times 10^{26} s^{-1}$ and $26 \times 10^{26} s^{-1}$. We note that the charge-exchange process in any case will lead to a modification of the energy distribution of the exospheric population since it favours, simultaneously the loss of cold populations and the gain of energetic ones. An accurate estimate of the spatial and temporal dependence of the exosphere loss as well as the determination of the O_2 energy distribution function resulting from the consideration of all loss processes, requires a detailed analytical or Direct Simulation Monte Carlo model (DSMC) and goes beyond the scope of this paper.

Table 6: Volume integrated O2 loss rates calculated through different models.

Model	**Smyth & Marconi (2006)** ($10^{26}s^{-1}$)	**(Shematovich et al., 2005)** ($10^{26}s^{-1}$)	**(Saur et al., 1998)** ($10^{26}s^{-1}$)	**(Dols et al., submitted)** ($10^{26}s^{-1}$)	**This work** ($10^{26}s^{-1}$)
***O_2* loss processes**					
Ionization		4.6[1,2] ; 5.3[3,2]	1.2	4.8	2.2 - 8.8[4,5]
Dissociation		0.039		3	1.3 - 5.3[4,6]
Charge-exchange	2.7	0.88[1] ; 0.014[3]	7.3	29.31	13 - 51[4,7,8]

[1] This value corresponds to Model D in Shematovich et al. (2005).
[2] This value includes ionization, charge-exchange and sweeping effects.
[3] This value corresponds to Model B in Shematovich et al. (2005).
[4] The lower and upper limits in the rates estimated in this work correspond to cases (a) and (b), respectively, for the considered O_2 exosphere (see text).
[5] Plasma conditions corresponding to Case (2) were considered (see Table 1).
[6] Plasma conditions corresponding to Case (3) were considered (see Table 1).
[7] The charge-exchange volume integrated rates in this work were estimated for the reaction $O_2^+ + O_2 \rightarrow O_2 + O_2^+$ which is the most effective one according to Table 4. The ionosphere O_2^+ density given by Sittler et al. (2013) was considered in the calculation.
[8] Assuming that at least half of the fresh energetic O_2 molecules produced through charge-exchange have velocities directions favoring escape, the net loss due to this process is expected to have values equal to 1/2 of the ones presented here (see also text).

As seen in Table 6, the O_2 volume integrated loss rates estimated in this study are by more than one order of magnitude larger than those calculated by Smyth & Marconi (2006) and by Shematovich et al. (2005). On the other hand, our results are consistent with those by Dols et al. (submitted). This is because contrary to past works (based on DSMC models), this study, as well as the study by Dols et al. (submitted), includes the charge exchange loss process between a high density ionospheric O_2^+ population and the exospheric O_2 considering energy dependent cross sections for the respective reactions. On the other hand, small differences between our estimated rates and those by Dols et al. (submitted) are due to the exosphere model used each time as a basis for the calculation (Dols et al. (submitted) used the atmosphere column densities by Saur et al. (1998) whereas we used the ones of EGEON, in Plainaki et al. (2013), revised due to yield corrections). On the other hand, Saur et al. (1998) estimated analytically the neutral losses due to both ionization and charge exchange. In order to make a comparison of the results presented in this paper and those in Saur et al. (1998), some clarifications of the vocabulary and the method used by these authors are necessary. Regarding ionization, what was actually calculated by Saur et al. (1998) was the flux of the ionized neutrals hitting the surface of Europa or being convected out of Europa's atmosphere. Such a process is referred to as "pick up loss" in that paper. Regarding

charge exchange, Saur et al. (1998) computed a flux of ions out of the exobase generated after a collision of an ion with a neutral. We note that in that calculation the authors considered only the charge exchange cross section, whereas the respective loss process was referred to as "atmospheric sputtering"[1]. On the basis of the above, it is reasonable to compare quantitatively our ionization and charge exchange results with the pick up loss and atmospheric sputtering results, respectively, presented in Table 2 in the Saur et al. (1998) paper. We find that the volume integrated ionization loss rate calculated by Saur et al. (1998) is consistent with our results. In addition, our net charge-exchange volume integrated loss rate (ranging from $6.5 \times 10^{26} s^{-1}$ to $26 \times 10^{26} s^{-1}$) is similar to the one of Saur et al. (1998), when considering the exosphere configuration case (a) (i.e. leading hemisphere is the illuminated one) and it is ~ 3 times larger in the exosphere configuration case (b) (i.e. trailing hemisphere is the illuminated one). Since the loss rate is proportional to the exosphere density, the difference between our results and those in Saur et al. (1998) can be explained on the basis of the combined effect of the neutral density assumed in each case and the considered cross sections. For the exosphere configuration case (a) the EGEON model gives a column density equal to $2.7 \times 10^{18} m^{-2}$, similar to the one assumed by Saur et al. (1998) (equal to $5 \times 10^{18} m^{-2}$) hence the averaged volume integrated loss rates are very similar. For the exosphere configuration case (b) the EGEON model gives a column density equal to $11 \times 10^{18} m^{-2}$ which is 2.2 times higher than the one assumed by Saur et al. (1998). We note that such a dense exosphere is the result of the effectiveness of the radiolysis process leading to a major surface release (and hence exosphere generation) when the trailing hemisphere of the moon is illuminated, as shown in Plainaki et al. (2013). Nevertheless, the obtained rates (see Table 6) are not strictly proportional since energy dependent cross section were considered in this study. Saur et al. (1998) assumed an effective charge exchange cross section value corresponding to an ion velocity of 60 km/s, equal to $2.6 \times 10^{-19} m^2$.

The main conclusion of the current study is that one of the dominant loss processes of Europa's exosphere is coming from the charge-exchange between the tenuous O_2 atmosphere and its own atmosphere ions. However, this rather unexpected result should be treated with caution due to uncertainties in the determination of the energy distribution function and density of the pickups ions due to limited in situ measurements. It is known that electron densities up to 104 cm^{-3} were measured very close to the moon's surface, however, the determination of the dominant ion species is still open. O_2^+ could be the main ion, but in the very near-surface layer the situation is rather complicated due to the following two reasons: 1) O_2^+ can be lost via its dissociative recombination with the ionospheric (thermal) electrons; and 2) ionization chemistry in the $O_2 + H_2 + H_2O$ mixtures results in the domination of the O_2^+, O_2H^+ and H_3O^+ ions (Larsson et al., 2012). Although H_2 and H_2O are minor species, nevertheless they should change the ion composition near surface. Such reactions could reduce our above estimated charge-exchange rates up to one order of magnitude.

The physics of plasma-moon interactions in the Jupiter system is one of the major interests of the international scientific community, especially in view of the upcoming JUICE mission (Grasset et al., 2013). The understanding of the spatial and temporal variability of Europa's neutral environment as well as of the implications of its interactions with the moon's internal ocean, require detailed knowledge of the neutral-plasma interactions. The related existing observations, obtained with HST (Hall et al., 1998; McGrath et al., 2004; Saur et al., 2011) and to a lesser extent in situ (Kliore et al.,

[1]Note that according to Johnson (1994) the term "atmospheric sputtering" should refer to the combination of many processes rather than a single one

1997; Kurth et al., 2001; Hansen et al., 2005), have provided important constraints for determining the exosphere generation and loss rates. However, a direct measurement of the main exospheric species has not been performed and these limited available observations are just proxies of the exosphere bulk constituents (e.g. OI UV emission is a proxy for O_2). Moreover, the existence of several exosphere models based on very different approaches (e.g. assuming either the collisional (e.g. Shematovich et al., 2005; Smyth & Marconi, 2006) or the collisionless (e.g. Cassidy et al., 2007; Plainaki et al., 2012) approximation, the existent of several plasma interaction models (e.g. Saur et al., 1998; Sittler et al., 2013; Dols et al., submitted) together with recent debates on the nature of Europa's neutral and plasma environments (see paper by Shemansky et al. (2014)) has resulted in a yet fragmentary understanding of Europa's plasma-neutral interactions. In view of the future JUICE mission observations, the need for an overall revision of the source and loss mechanisms for the exosphere of Europa is urgent. In this context, we provided in the current study a rough estimation of the efficiency of the dominant interactions at Europa that can be used as a starting point in future modeling studies of the moon's environment. Such models could be used as basic tools for planning the future JUICE observations and, later, for interpreting the actual exosphere and plasma measurements.

4. Conclusion

In the current study the loss rates of the main components of Europa's exosphere (O_2, H_2O, H_2) were estimated on the basis of energy-dependent reaction cross sections found in literature and, for the first time, updated plasma conditions obtained from the recent state to the art model by Bagenal et al. (2015). We performed calculations for electron impact dissociation and ionization processes, for charge-exchange (considering plasma torus, pick up and ionosphere ions) and for photo processes (for both cases of quite and active Sun). For the dominant (in the near-surface regions) O_2 species, the volume integrated loss rates were estimated, using the revised (for the surface release yields) O_2 exosphere described by the EGEON model, for two different configuration between Europa, Jupiter and the Sun (i.e. subsolar point coincides with the leading hemisphere apex and subsolar point coincides with the trailing hemisphere apex) (Plainaki et al., 2013). The results of the comparison of the rates provided in this paper with the ones in other studies can be summarized as follows:

1. For both H_2O and H_2 exospheres, the loss is very variable depending on the position of Europa with respect to the JPS. The cold plasma electron population is the main responsible for H_2O and H_2 loss, in particular maximum loss is expected under median plasma conditions and median or high plasma conditions for H_2O and H_2 respectively.
2. For the O_2 exosphere, we find the $O_2 - O_2^+$ charge-exchange process may have a dominant role in the exosphere loss, contrary to what it had been previously thought. Using the revised O_2 column density based on the estimation from the EGEON model (Plainaki et al., 2013), we estimate that the $O_2 - O_2^+$ charge transfer rate is in the range $(13 - 51) \times 10^{26} s^{-1}$, depending also on the configuration between Europa, Jupiter and the Sun.

The estimations provided in this paper could be of help while modeling the Galilean moons, environments providing constrains for the neutral-ion balance and the surface release from ice. In view of the future JUICE mission, these estimates could be useful in order to plan observation strategies and, later, interpret the mission measurements.

Acknowledgements

The work in this paper has been performed in the context of the activities of the ISSI International Team #322: "Towards a global unified model of Europa's exosphere in view of the JUICE mission" http://www.issibern.ch/teams/exospherejuice/".

This research was supported by the Italian Space Agency (ASI) through the ASI-INAF agreement no.2013-056-RO.

References

Anicich, V. G., & McEwan, M. J. (1997). Ion-molecule chemistry in Titan's ionosphere. Planet. Space Sci., *45*, 897–921. doi:10.1016/S0032-0633(97)00053-6.

Bagenal, F. (1994). Empirical model of the Io plasma torus: Voyager measurements. J. Geophys. Res., *99*, 11043–11062. doi:10.1029/93JA02908.

Bagenal, F., Dowling, T. E., & McKinnon, W. B. (2004). *Jupiter*.

Bagenal, F., Shemansky, D. E., McNutt, R. L., Jr., Schreier, R., & Eviatar, A. (1992). The abundance of O(2+) in the Jovian magnetosphere. Geophys. Res. Lett., *19*, 79–82. doi:10.1029/92GL00070.

Bagenal, F., Sidrow, E., Wilson, R. J., Cassidy, T. A., Dols, V., Crary, F. J., Steffl, A. J., Delamere, P. A., Kurth, W. S., & Paterson, W. R. (2015). Plasma conditions at Europa's orbit. Icarus, *261*, 1–13. doi:10.1016/j.icarus.2015.07.036.

Barabash, S., Lukyanov, A. V., C:son Brandt, P., & Lundin, R. (2001). Energetic neutral atom imaging of Mercury's magnetosphere 3. Simulated images and instrument requirements. Planet. Space Sci., *49*, 1685–1692. doi:10.1016/S0032-0633(01)00107-6.

Baragiola, R. A. (2003). Water ice on outer solar system surfaces: Basic properties and radiation effects. Planet. Space Sci., *51*, 953–961. doi:10.1016/j.pss.2003.05.007.

Benyoucef, D., & Yousfi, M. (2014). Ar + /ar, o 2 + /o 2 and n 2 + /n 2 elastic momentum collision cross sections: Calculation and validation using the semi-classical model. *Plasma Science and Technology*, *16*, 588. URL: http://stacks.iop.org/1009-0630/16/i=6/a=09.

Brown, M. E. (2001). Potassium in Europa's Atmosphere. Icarus, *151*, 190–195. doi:10.1006/icar.2001.6612.

Brown, M. E., & Hill, R. E. (1996). Discovery of an extended sodium atmosphere around Europa. Nature, *380*, 229–231. doi:10.1038/380229a0.

Brown, W. L., Lanzerotti, L. J., & Johnson, R. E. (1982). Fast Ion Bombardment of Ices and its Astrophysical Implications. *Science*, *218*, 525–531. doi:10.1126/science.218.4572.525.

Brown, W. L., Lanzerotti, L. J., Poate, J. M., & Augustyniak, W. M. (1978). "sputtering" of ice by mev light ions. *Phys. Rev. Lett.*, *40*, 1027–1030. URL: http://link.aps.org/doi/10.1103/PhysRevLett.40.1027. doi:10.1103/PhysRevLett.40.1027.

Burger, M. H., & Johnson, R. E. (2004). Europa's neutral cloud: morphology and comparisons to Io. Icarus, *171*, 557–560. doi:10.1016/j.icarus.2004.06.014.

Burger, M. H., Wagner, R., Jaumann, R., & Cassidy, T. A. (2010). Effects of the External Environment on Icy Satellites. Space Sci. Rev., *153*, 349–374. doi:10.1007/s11214-010-9645-z.

Cassidy, T., Coll, P., Raulin, F., Carlson, R. W., Johnson, R. E., Loeffler, M. J., Hand, K. P., & Baragiola, R. A. (2010). Radiolysis and Photolysis of Icy Satellite Surfaces: Experiments and Theory. Space Sci. Rev., *153*, 299–315. doi:10.1007/s11214-009-9625-3.

Cassidy, T. A., Johnson, R. E., Geissler, P. E., & Leblanc, F. (2008). Simulation of Na D emission near Europa during eclipse. *Journal of Geophysical Research (Planets)*, *113*, 2005. doi:10.1029/2007JE002955.

Cassidy, T. A., Johnson, R. E., McGrath, M. A., Wong, M. C., & Cooper, J. F. (2007). The spatial morphology of Europa's near-surface O $_2$ atmosphere. Icarus, *191*, 755–764. doi:10.1016/j.icarus.2007.04.033.

Cassidy, T. A., Paranicas, C. P., Shirley, J. H., Dalton, J. B., III, Teolis, B. D., Johnson, R. E., Kamp, L., & Hendrix, A. R. (2013). Magnetospheric ion sputtering and water ice grain size at Europa. Planet. Space Sci., *77*, 64–73. doi:10.1016/j.pss.2012.07.008.

Coplan, M. A., & Ogilvie, K. W. (1970). Charge Exchange for H^+ and H^+_2 in H_2O, CO_2, and NH_3. J. Chem. Phys., *52*, 4154–4160. doi:10.1063/1.1673624.

Cosby, P. C. (1993). Electron-impact dissociation of oxygen. J. Chem. Phys., *98*, 9560–9569. doi:10.1063/1.464387.

Coustenis, A., Tokano, T., Burger, M. H., Cassidy, T. A., Lopes, R. M., Lorenz, R. D., Retherford, K. D., & Schubert, G. (2010). Atmospheric/Exospheric Characteristics of Icy Satellites. Space Sci. Rev., *153*, 155–184. doi:10.1007/s11214-009-9615-5.

Daglis, I. A., & Livi, S. (1995). Potential merits for substorm research from imaging of charge-exchange neutral atoms. *Annales Geophysicae*, *13*, 505–516. doi:10.1007/s00585-995-0505-1.

Dalton, J. B., Cruikshank, D. P., Stephan, K., McCord, T. B., Coustenis, A., Carlson, R. W., & Coradini, A. (2010). Chemical Composition of Icy Satellite Surfaces. Space Sci. Rev., *153*, 113–154. doi:10.1007/s11214-010-9665-8.

De La Haye, V. (2005). *Formation and heating efficiencies in Titan's upper atmosphere: Construction of a coupled Io, neutral and thermal structure model to interpret the first INMS Cassini data*. Ph.D. thesis University of Michigan.

Delamere, P. A., Bagenal, F., & Steffl, A. (2005). Radial variations in the Io plasma torus during the Cassini era. *Journal of Geophysical Research (Space Physics)*, *110*, 12223. doi:10.1029/2005JA011251.

Dols, V., Bagenal, F., Cassidy, T., Crary, F., & Delamare, P. (submitted). Europa's Atmospheric Neutral Escape: Importance of Symmetrical O_2 Charge Exchange, .

Fehsenfeld, F. C., Schmeltekopf, A. L., & Ferguson, E. E. (1967). Thermal-Energy IonNeutral Reaction Rates. VII. Some Hydrogen-Atom Abstraction Reactions. J. Chem. Phys., *46*, 2802–2808. doi:10.1063/1.1841117.

Galli, A., Pommerol, A., Vorburger, A., Wurz, P., Tulej, M., Scheer, J., Thomas, N., Wieser, M., & Barabash, S. (2015). The first laboratory measurements of sulfur ions sputtering water ice. In *EGU2015-3752*.

Grasset, O., Dougherty, M., Coustenis, A., Bunce, E., Erd, C., Titov, D., Blanc, M., Coates, A., Drossart, P., Fletcher, L., Hussmann, H., Jaumann, R., Krupp, N., Lebreton, J.-P., Prieto-Ballesteros, O., Tortora, P., Tosi, F., & Van, H. T. (2013). Jupiter icy moons explorer (juice):

An esa mission to orbit ganymede and to characterise the jupiter system. *PLANETARY AND SPACE SCIENCE*, *78*, 1–21. URL: http://dx.doi.org/10.1016/j.pss.2012.12.002. doi:10.1016/j.pss.2012.12.002.

Gurnett, D. A., Kurth, W. S., Roux, A., Bolton, S. J., Thomsen, E. A., & Groene, J. B. (1998). Galileo plasma wave observations near Europa. Geophys. Res. Lett., *25*, 237–240. doi:10.1029/97GL03706.

Hall, D. T., Feldman, P. D., McGrath, M. A., & Strobel, D. F. (1998). The Far-Ultraviolet Oxygen Airglow of Europa and Ganymede. ApJ, *499*, 475–481. doi:10.1086/305604.

Hall, D. T., Strobel, D. F., Feldman, P. D., McGrath, M. A., & Weaver, H. A. (1995). Detection of an oxygen atmosphere on Jupiter's moon Europa. Nature, *373*, 677–679. doi:10.1038/373677a0.

Hansen, C. J., Shemansky, D. E., & Hendrix, A. R. (2005). Cassini UVIS observations of Europa's oxygen atmosphere and torus. Icarus, *176*, 305–315. doi:10.1016/j.icarus.2005.02.007.

Harb, T., Kedzierski, W., & McConkey, J. W. (2001a). Production of ground state OH following electron impact on H_2O. J. Chem. Phys., *115*, 5507–5512. doi:10.1063/1.1397327.

Harb, T., Kedzierski, W., & McConkey, W. J. (2001b). Dissociation of Water by Electron Impact. In *APS Division of Atomic, Molecular and Optical Physics Meeting Abstracts* (p. 5026).

Hasan, A. T., & Gray, T. J. (2007). Electron-Capture Cross Sections of Ground-State O2+ Recoil Ions in Slow Collisions with H2 and O2. *International Journal of Molecular Sciences*, (pp. 1158–1164).

Hasted, J. B., & Hussain, M. (1964). Electron capture by multiply charged ions. *Proceedings of the Physical Society*, *83*, 911–924. doi:10.1088/0370-1328/83/6/303.

Hubert, B., Gérard, J.-C., Gustin, J., Bisikalo, D. V., Shematovich, V. I., & Gladstone, G. R. (2012). Cassini-UVIS observation of dayglow FUV emissions of carbon in the thermosphere of Venus. Icarus, *220*, 635–646. doi:10.1016/j.icarus.2012.06.002.

Huebner, W. F., Keady, J. J., & Lyon, S. P. (1992). Solar photo rates for planetary atmospheres and atmospheric pollutants. Ap&SS, *195*, 1–289. doi:10.1007/BF00644558.

Ionov, D. E., Bisikalo, D. V., Shematovich, V. I., & Huber, B. (2014). Ionization fraction in the thermosphere of the exoplanet HD 209458b. *Solar System Research*, *48*, 105–112. doi:10.1134/S0038094614020026.

Irvine, A. D., & Latimer, C. J. (1997). Charge-exchange processes involving ground- and excited-state O2+ and H2+ ions with H2 and O2. *International Journal of Mass Spectrometry and Ion Processes*, *164*, 115–120. doi:10.1016/S0168-1176(97)00025-6.

Itikawa, Y. (2009). Cross sections for electron collisions with oxygen molecules. *Journal of Physical and Chemical Reference Data*, *38*.

Itikawa, Y., & Mason, N. (2005). Cross Sections for Electron Collisions with Water Molecules. *Journal of Physical and Chemical Reference Data*, *34*, 1–22. doi:10.1063/1.1799251.

Johnson, P. V., & Kanik, I. (2001). Inelastic differential electron scattering cross sections of molecular oxygen (O_2) in the 20-100 eV impact energy range. *Journal of Physics B Atomic Molecular Physics*, *34*, 3041–3051. doi:10.1088/0953-4075/34/15/310.

Johnson, R. E. (1990). *Energetic Charged-Particle Interactions with Atmospheres and Surfaces*.

Johnson, R. E. (1994). Plasma-Induced Sputtering of an Atmosphere. Space Sci. Rev., *69*, 215–253. doi:10.1007/BF02101697.

Johnson, R. E. (2000). NOTE: Sodium at Europa. Icarus, *143*, 429–433. doi:10.1006/icar.1999.6327.

Johnson, R. E., Luhmann, J. G., Tokar, R. L., Bouhram, M., Berthelier, J. J., Sittler, E. C., Cooper, J. F., Hill, T. W., Smith, H. T., Michael, M., Liu, M., Crary, F. J., & Young, D. T. (2006). Production, ionization and redistribution of O $_2$ in Saturn's ring atmosphere. Icarus, *180*, 393–402. doi:10.1016/j.icarus.2005.08.021.

Johnston, A. R., & Burrow, P. D. (1995). Electron-impact ionization of na. *Phys. Rev. A*, *51*, R1735–R1737. URL: http://link.aps.org/doi/10.1103/PhysRevA.51.R1735. doi:10.1103/PhysRevA.51.R1735.

Kabin, K., Combi, M. R., Gombosi, T. I., Nagy, A. F., DeZeeuw, D. L., & Powell, K. G. (1999). On Europa's magnetospheric interaction: A MHD simulation of the E4 flyby. J. Geophys. Res., *104*, 19983–19992. doi:10.1029/1999JA900263.

Kim, J. K., & Huntress, W. T., Jr. (1975). Ion cyclotron resonance studies on the reaction of H_2^+ and D_2^+ ions with various simple molecules and hydrocarbons. J. Chem. Phys., *62*, 2820–2825. doi:10.1063/1.430817.

Kimmel, G. A., Orlando, T. M., Vézina, C., & Sanche, L. (1994). Low-energy electron-stimulated production of molecular hydrogen from amorphous water ice. J. Chem. Phys., *101*, 3282–3286. doi:10.1063/1.468430.

Kivelson, M. G., Bagenal, F., Kurth, W. S., Neubauer, F. M., Paranicas, C., & Saur, J. (2004). Magnetospheric interactions with satellites. In F. Bagenal, T. E. Dowling, & W. B. McKinnon (Eds.), *Jupiter. The Planet, Satellites and Magnetosphere* (pp. 513–536).

Kivelson, M. G., Khurana, K. K., & Volwerk, M. (2009). Europa's Interaction with the Jovian Magnetosphere. In R. T. Pappalardo, W. B. McKinnon, & K. K. Khurana (Eds.), *Europa, Edited by Robert T. Pappalardo, William B. McKinnon, Krishan K. Khurana ; with the assistance of René Dotson with 85 collaborating authors. University of Arizona Press, Tucson, 2009. The University of Arizona space science series ISBN: 9780816528448, p.545* (p. 545).

Kliore, A. J., Hinson, D. P., Flasar, F. M., Nagy, A. F., & Cravens, T. E. (1997). The ionosphere of Europa from Galileo radio occultations. *Science*, *277*, 355–358. doi:10.1126/science.277.5324.355.

Krupp, N., Khurana, K. K., Iess, L., Lainey, V., Cassidy, T. A., Burger, M., Sotin, C., & Neubauer, F. (2010). Environments in the Outer Solar System. Space Sci. Rev., *153*, 11–59. doi:10.1007/s11214-010-9653-z.

Kurth, W. S., Gurnett, D. A., Persoon, A. M., Roux, A., Bolton, S. J., & Alexander, C. J. (2001). The plasma wave environment of Europa. Planet. Space Sci., *49*, 345–363. doi:10.1016/S0032-0633(00)00156-2.

Larsson, M., Geppert, W. D., & Nyman, G. (2012). Ion chemistry in space. *Reports on Progress in Physics*, *75*, 066901. URL: http://stacks.iop.org/0034-4885/75/i=6/a=066901.

Leblanc, F., Johnson, R. E., & Brown, M. E. (2002). Europa's Sodium Atmosphere: An Ocean Source? Icarus, *159*, 132–144. doi:10.1006/icar.2002.6934.

Leblanc, F., Potter, A. E., Killen, R. M., & Johnson, R. E. (2005). Origins of Europa Na cloud and torus. Icarus, *178*, 367–385. doi:10.1016/j.icarus.2005.03.027.

Lindsay, B., & Mangan, M. (2003). 5.1 ionization. In Y. Itikawa (Ed.), *Interactions of Photons and Electrons with Molecules* (pp. 5001–5077). Springer Berlin Heidelberg volume 17C of *Landolt-Brnstein - Group I Elementary Particles, Nuclei and Atoms*. URL: http://dx.doi.org/10.1007/10874891_2. doi:10.1007/10874891_2.

Lipatov, A. S., Cooper, J. F., Paterson, W. R., Sittler, E. C., Hartle, R. E., & Simpson, D. G. (2010). Jovian plasma torus interaction with Europa: 3D hybrid kinetic simulation. First results. Planet. Space Sci., *58*, 1681–1691. doi:10.1016/j.pss.2010.06.015.

Lipatov, A. S., Cooper, J. F., Paterson, W. R., Sittler, E. C., Jr., Hartle, R. E., & Simpson, D. G. (2013). Jovian plasma torus interaction with Europa. Plasma wake structure and effect of inductive magnetic field: 3D hybrid kinetic simulation. Planet. Space Sci., *77*, 12–24. doi:10.1016/j.pss.2013.01.009. arXiv:1212.3626.

Lishawa, C. R., Dressler, R. A., Gardner, J. A., Salter, R. H., & Murad, E. (1990). Cross sections and product kinetic energy analysis of H_2O^+-H_2O collisions at suprathermal energies. J. Chem. Phys., *93*, 3196–3206. doi:10.1063/1.458852.

McGrath, M. A., & Johnson, R. E. (1989). Charge exchange cross sections for the io plasma torus. *Journal of Geophysical Research: Space Physics*, *94*, 2677–2683. URL: http://dx.doi.org/10.1029/JA094iA03p02677. doi:10.1029/JA094iA03p02677.

McGrath, M. A., Lellouch, E., Strobel, D. F., Feldman, P. D., & Johnson, R. E. (2004). Satellite atmospheres. In F. Bagenal, T. E. Dowling, & W. B. McKinnon (Eds.), *Jupiter. The Planet, Satellites and Magnetosphere* (pp. 457–483).

Milillo, A., Orsini, S., & Daglis, I. A. (2001). Empirical model of proton fluxes in the equatorial inner magnetosphere: Development. J. Geophys. Res., *106*, 25713–25730. doi:10.1029/2000JA900158.

Milillo, A., Plainaki, C., De Angelis, E., Mangano, V., Massetti, S., Mura, A., Orsini, S., & Rispoli, R. (submitted). Analytical model of Europa's O2 exosphere. Planet. Space Sci., .

Milillo, A., Wurz, P., Orsini, S., Delcourt, D., Kallio, E., Killen, R. M., Lammer, H., Massetti, S., Mura, A., Barabash, S., Cremonese, G., Daglis, I. A., Angelis, E., Lellis, A. M., Livi, S., Mangano, V., & Torkar, K. (2005). Surface-Exosphere-Magnetosphere System Of Mercury. Space Sci. Rev., *117*, 397–443. doi:10.1007/s11214-005-3593-z.

Möhlmann, G. R., & de Heer, F. J. (1979). Production of Balmer radiation by electron impact (0 2000 eV) on small hydrogen containing molecules. *Chemical Physics*, *40*, 157–162. doi:10.1016/0301-0104(79)85129-0.

Morgan, H. D., & Mentall, J. E. (1974). VUV dissociative excitation cross sections of H_2O, NH_3, and CH_4 by electron impact. J. Chem. Phys., *60*, 4734–4739. doi:10.1063/1.1680975.

Morrison, D., & Samz, J. (1980). *Voyage to Jupiter*.

Orlando, T. M., & Kimmel, G. A. (1997). The role of excitons and substrate temperature in low-energy (5-50 eV) electron-stimulated dissociation of amorphous D $_2$O ice. *Surface Science*, *390*, 79–85. doi:10.1016/S0039-6028(97)00511-6.

Orsini, S., & Milillo, A. (1999). Magnetospheric plasma loss processes in the Earth's ring current and energetic neutral atoms. *Nuovo Cimento C Geophysics Space Physics C*, *22*, 633–648.

Orsini, S., Milillo, A., Angelis, E. D., Lellis, A. M. D., Zanza, V., & Livi, S. (2001). Remote sensing of Mercury's magnetospheric plasma environment via energetic neutral atoms imaging. Planet. Space Sci., *49*, 1659–1668. doi:10.1016/S0032-0633(01)00104-0.

Pappalardo, R. T., McKinnon, W. B., & Khurana, K. K. (2009). *Europa*.

Paranicas, C., Cheng, A. F., & Williams, D. J. (1998). Inference of Europa's conductance from the Galileo Energetic Particles Detector. J. Geophys. Res., *103*, 15001–15008. doi:10.1029/98JA00961.

Plainaki, C., Milillo, A., Massetti, S., Mura, A., Jia, X., Orsini, S., Mangano, V., De Angelis, E., & Rispoli, R. (2015). The H_2O and O_2 exospheres of Ganymede: The result of a complex interaction between the jovian magnetospheric ions and the icy moon. Icarus, *245*, 306–319. doi:10.1016/j.icarus.2014.09.018.

Plainaki, C., Milillo, A., Mura, A., Orsini, S., & Cassidy, T. (2010). Neutral particle release from Europa's surface. Icarus, *210*, 385–395. doi:10.1016/j.icarus.2010.06.041. arXiv:0911.4602.

Plainaki, C., Milillo, A., Mura, A., Orsini, S., Massetti, S., & Cassidy, T. (2012). The role of sputtering and radiolysis in the generation of Europa exosphere. Icarus, *218*, 956–966. doi:10.1016/j.icarus.2012.01.023.

Plainaki, C., Milillo, A., Mura, A., Saur, J., Orsini, S., & Massetti, S. (2013). Exospheric O_2 densities at Europa during different orbital phases. Planet. Space Sci., *88*, 42–52. doi:10.1016/j.pss.2013.08.011.

Roelof, E. C. (1987). Energetic neutral atom image of a storm-time ring current. Geophys. Res. Lett., *14*, 652–655. doi:10.1029/GL014i006p00652.

Roelof, E. C., Mitchell, D. G., & Williams, D. J. (1985). Energetic neutral atoms (E approximately 50 keV) from the ring current - IMP 7/8 and ISEE 1. J. Geophys. Res., *90*, 10991. doi:10.1029/JA090iA11p10991.

Roth, L., Saur, J., Retherford, K. D., Strobel, D. F., Feldman, P. D., McGrath, M. A., & Nimmo, F. (2014). Transient Water Vapor at Europa's South Pole. *Science*, *343*, 171–174. doi:10.1126/science.1247051.

Rubin, M., Jia, X., Altwegg, K., Combi, M. R., Daldorff, L. K. S., Gombosi, T. I., Khurana, K., Kivelson, M. G., Tenishev, V. M., Tóth, G., Holst, B., & Wurz, P. (2015). Self-consistent multifluid MHD simulations of Europa's exospheric interaction with Jupiter's magnetosphere. *Journal of Geophysical Research (Space Physics)*, *120*, 3503–3524. doi:10.1002/2015JA021149.

Saur, J., Duling, S., Roth, L., Jia, X., Strobel, D. F., Feldman, P. D., Christensen, U. R., Retherford, K. D., McGrath, M. A., Musacchio, F., Wennmacher, A., Neubauer, F. M., Simon, S., & Hartkorn, O. (2015). The search for a subsurface ocean in Ganymede with Hubble Space Telescope observations of its auroral ovals. *Journal of Geophysical Research (Space Physics)*, *120*, 1715–1737. doi:10.1002/2014JA020778.

Saur, J., Feldman, P. D., Roth, L., Nimmo, F., Strobel, D. F., Retherford, K. D., McGrath, M. A., Schilling, N., Gérard, J.-C., & Grodent, D. (2011). Hubble Space Telescope/Advanced Camera for Surveys Observations of Europa's Atmospheric Ultraviolet Emission at Eastern Elongation. ApJ, *738*, 153. doi:10.1088/0004-637X/738/2/153.

Saur, J., Strobel, D. F., & Neubauer, F. M. (1998). Interaction of the Jovian magnetosphere with Europa: Constraints on the neutral atmosphere. J. Geophys. Res., *103*, 19947–19962. doi:10.1029/97JE03556.

Schilling, N., Neubauer, F. M., & Saur, J. (2007). Time-varying interaction of Europa with the jovian magnetosphere: Constraints on the conductivity of Europa's subsurface ocean. Icarus, *192*, 41–55. doi:10.1016/j.icarus.2007.06.024.

Schilling, N., Neubauer, F. M., & Saur, J. (2008). Influence of the internally induced magnetic field on the plasma interaction of Europa. *Journal of Geophysical Research (Space Physics)*, *113*, 3203. doi:10.1029/2007JA012842.

Shemansky, D. E. (1987). Ratio of oxygen to sulfur in the Io plasma torus. J. Geophys. Res., *92*, 6141–6146. doi:10.1029/JA092iA06p06141.

Shemansky, D. E., Yung, Y. L., Liu, X., Yoshii, J., Hansen, C. J., Hendrix, A. R., & Esposito, L. W. (2014). A New Understanding of the Europa Atmosphere and Limits on Geophysical Activity. ApJ, *797*, 84. doi:10.1088/0004-637X/797/2/84.

Shematovich, V. I., Johnson, R. E., Cooper, J. F., & Wong, M. C. (2005). Surface-bounded atmosphere of Europa. Icarus, *173*, 480–498. doi:10.1016/j.icarus.2004.08.013.

Shirai, T., Tabata, T., & Tawara, T. (2001). Analytic cross sections for electron collisions with CO, CO_2, and H_2O relevant to edge plasma impurities. *Atomic Data and Nuclear Data Tables*, *79*, 143–184. URL: http://www.sciencedirect.com/science/article/pii/S0092640X01908666. doi:http://dx.doi.org/10.1006/adnd.2001.0866.

Sittler, E. C., Cooper, J. F., Hartle, R. E., Paterson, W. R., Christian, E. R., Lipatov, A. S., Mahaffy, P. R., Paschalidis, N. P., Coplan, M. A., Cassidy, T. A., Richardson, J. D., Fegley, B., & Andre, N. (2013). Plasma ion composition measurements for Europa. Planet. Space Sci., *88*, 26–41. doi:10.1016/j.pss.2013.01.013.

Sittler, E. C., & Strobel, D. F. (1987). Io plasma torus electrons - Voyager 1. J. Geophys. Res., *92*, 5741–5762. doi:10.1029/JA092iA06p05741.

Smyth, W. H., & Combi, M. R. (1997). Io's Sodium Corona and Spatially Extended Cloud: A Consistent Flux Speed Distribution. Icarus, *126*, 58–77. doi:10.1006/icar.1996.5633.

Smyth, W. H., & Marconi, M. L. (2006). Europa's atmosphere, gas tori, and magnetospheric implications. Icarus, *181*, 510–526. doi:10.1016/j.icarus.2005.10.019.

Stebbings, R. F., Smith, A. C. H., & Ehrhardt, H. (1964). Charge Transfer between Oxygen Atoms and O^+ and H^+ Ions. J. Geophys. Res., *69*, 2349–2355. doi:10.1029/JZ069i011p02349.

Steffl, A. J., Bagenal, F., & Stewart, A. I. F. (2004). Cassini UVIS observations of the Io plasma torus. II. Radial variations. Icarus, *172*, 91–103. doi:10.1016/j.icarus.2004.04.016. arXiv:1301.3813.

Straub, H. C., Renault, P., Lindsay, B. G., Smith, K. A., & Stebbings, R. F. (1996). Absolute partial cross sections for electron-impact ionization of H_2, N_2, and O_2 from threshold to 1000 eV. Phys. Rev. A, *54*, 2146–2153. doi:10.1103/PhysRevA.54.2146.

Tawara, H., Kato, T., & Nakai, Y. (1985). Cross Sections for Electron Capture and Loss by Positive Ions in Collisions with Atomic and Molecular Hydrogen. *Atomic Data and Nuclear Data Tables*, *32*, 235. doi:10.1016/0092-640X(85)90007-5.

Teolis, B. D., Niemann, H. B., Waite, J. H., Gell, D. A., Perryman, R. S., Kasprzak, W. T., Mandt, K. E., Yelle, R. V., Lee, A. Y., Pelletier, F. J., Miller, G. P., Young, D. T., Bell, J. M., Magee, B. A., Patrick, E. L., Grimes, J., Fletcher, G. G., & Vuitton, V. (2015). A Revised Sensitivity Model for Cassini INMS: Results at Titan. Space Sci. Rev., . doi:10.1007/s11214-014-0133-8.

Turner, B. R., & Rutherford, J. A. (1968). Charge transfer and ion-atom interchange reactions of water vapor ions. J. Geophys. Res., *73*, 6751–6758. doi:10.1029/JA073i021p06751.

Vance, D. W., & Bailey, T. L. (1966). Inelastic Collisions of $H^+{}_2$ and $N^+{}_2$ Ions with Hydrogen Molecules. J. Chem. Phys., *44*, 486–493. doi:10.1063/1.1726714.

Watanabe, N., Horii, T., & Kouchi, A. (2000). Measurements of D_2 Yields from Amorphous D_2O Ice by Ultraviolet Irradiation at 12 K. ApJ, *541*, 772–778. doi:10.1086/309458.

Yoon, J.-S., Song, M.-Y., Han, J.-M., Hwang, S. H., Chang, W.-S., Lee, B., & Itikawa, Y. (2008). Cross Sections for Electron Collisions with Hydrogen Molecules. *Journal of Physical and Chemical Reference Data*, *37*, 913–931. doi:10.1063/1.2838023.